Diffusion of iron and nickel in single-crystalline copper

A. Almazouzi*
Institut für Physikalische Chemie, Freie Universität Berlin, Takustrasse 3, D-14195 Berlin, Germany

M.-P. Macht and V. Naundorf
Hahn-Meitner-Institut Berlin, Glienickerstrasse 100, D-14109 Berlin, Germany

G. Neumann
Institut für Physikalische Chemie, Freie Universität Berlin, Takustrasse 3, D-14195 Berlin, Germany
(Received 22 December 1995)

The diffusion of Fe and Ni in single-crystalline copper was investigated in the temperature range from 651 to 870 K and from 613 to 949 K, respectively. Ion-beam sputtering in combination with secondary-ion mass spectrometry was employed to measure concentration depth profiles. The temperature dependence of the diffusion coefficients of Fe and Ni in copper can be described by $D_{\mathrm{Fe}}=(0.10\pm0.03)\times10^{-4}\exp(-2.04\pm0.02$ eV/kT) m^2 s^{-1} and $D_{\mathrm{Ni}}=(0.62^{+0.31}_{-0.21})\times10^{-4}\exp(-2.32\pm0.025$ eV/kT) m^2 s^{-1}. These results are compatible with earlier high-temperature tracer data. A combination of those with the present low-temperature data reveals a curvature in the respective Arrhenius plots. This curvature is ascribed to the contribution of divacancies at high temperatures. The temperature functions of D_{Fe} and D_{Ni} can be described with the aid of the modified electrostatic model of impurity diffusion, assuming effective values for the charge difference between host atom and impurity. [S0163-1829(96)00126-9]

I. INTRODUCTION

Recently, a modified electrostatic model for the diffusion of electropositive impurities in noble metals was proposed.[1] This approach is based on the assumptions of the five-frequency model of impurity diffusion.[2] It combines the essentials of the original electrostatic model (E model;[3] Lazarus[4] earlier considered an electrostatic interaction between impurity and vacancy) and of the thermodynamic model (T_m model[5,6]) and takes into account the contribution of divacancies at higher temperatures.[7] As a consequence of contributions from both monovacancies ($1V$) and divacancies ($2V$) with different diffusion energies Q_{1V} and Q_{2V} a curved Arrhenius plot ($\ln D$ vs $1/T$) of the diffusion coefficient D is expected, viz.,

$$D=D_{1V}+D_{2V}=D_{1V}^{0}\exp(-Q_{1V}/kT)+D_{2V}^{0}\exp(-Q_{2V}/kT). \quad (1)$$

The T_m model and the original E model were unable to describe the diffusion of groups IV to VII metals (Ti to Mn) in noble metals.[3,5,6] On the other hand, the application of the T_m model to the group VIII metals led to an acceptable agreement between experimental and calculated diffusion energies,[5] and even the original E model could explain the diffusion energies of Fe, Co, and Ni in copper by use of effective charges of the impurities.[3] The modified electrostatic model should, in principle, be applicable to the diffusion of the whole range of groups III to VIII metals, provided theoretically well-founded effective charges are available.

In the present paper investigations on the diffusion of Fe and Ni in single-crystalline copper are reported. The diffusion experiments were performed in the temperature range between 651 and 870 K and between 613 and 949 K, respectively. Diffusion parameters were obtained from the measurement of the concentration depth profiles by means of the ion-beam sputtering technique combined with secondary-ion mass spectrometry (SIMS).[8] The aims of the present investigation are (i) to quantitatively determine any curvature of the Arrhenius plots, and (ii) to test the applicability of the modified electrostatic model of impurity diffusion to group VIII metals in copper.

II. EXPERIMENTAL PROCEDURE

Measurements were performed on single-crystalline sandwich specimens[8] with a thin inserted layer of Fe and Ni, respectively. The specimens were prepared from 99.999% copper single crystals with a dislocation density of about 10^{11} m^{-2}. Slices with 10 mm diameter, about 0.5 mm thick, were spark cut from these crystals and one surface of each slice was carefully mechanically polished. Thereafter a layer of about 100 μm thickness was removed by electrolytic polishing to eliminate the deformed zone and to get a smooth surface. This surface was sputter cleaned for about 1 h with 4 keV Ar^+ ions in an UHV chamber. Subsequently, about 0.2 μg/cm^2 Fe and less than 1 μg/cm^2 Ni were sputter deposited onto it; this is the equivalent of some monolayers of the impurity. Finally, the impurity layer was covered by an epitaxial copper layer of 50–200 nm by controlled vapor deposition at room temperature, without breaking the vacuum.

The specimens were diffusion annealed either in high vacuum of better than 10^{-4} Pa or in Ar/6.2% H_2 atmosphere. In the temperature range between 613 and 949 K the annealing time was varied between about 65 and 2.5×10^6 s. The temperatures were measured by a NiCr/Ni thermocouple

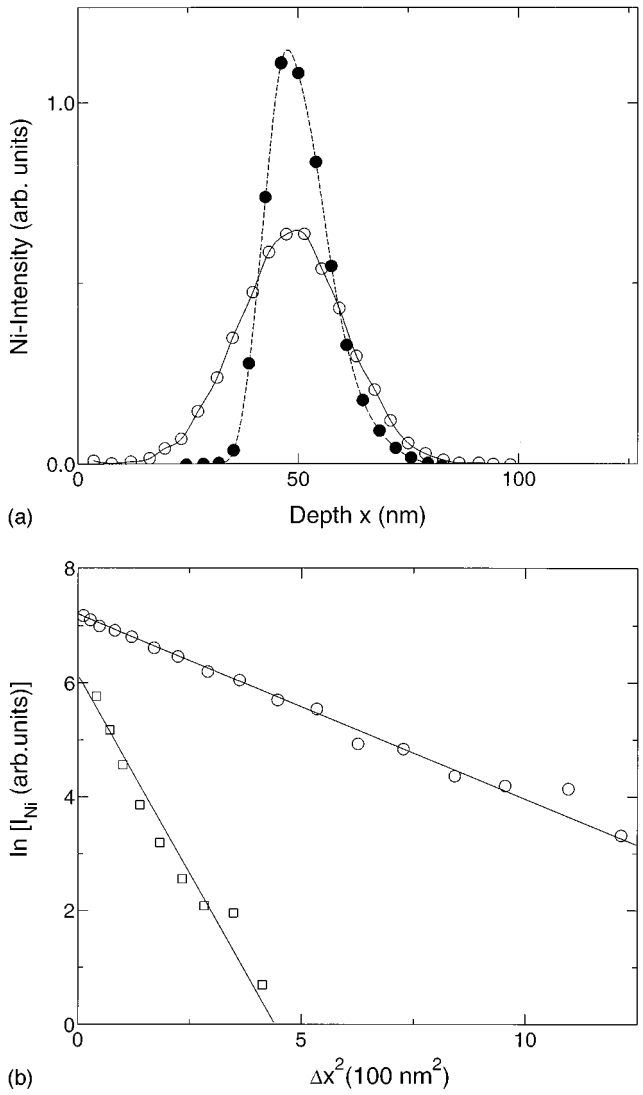

FIG. 1. (a) Typical depth profile of a Cu/Ni/Cu sandwich specimen (full line, after diffusion annealing for 73.4 s at 849 K; dashed line, as prepared). (b) Gaussian plot [ln$c$ vs Δx^2, cf. Eq. (2) of text] of the same data.

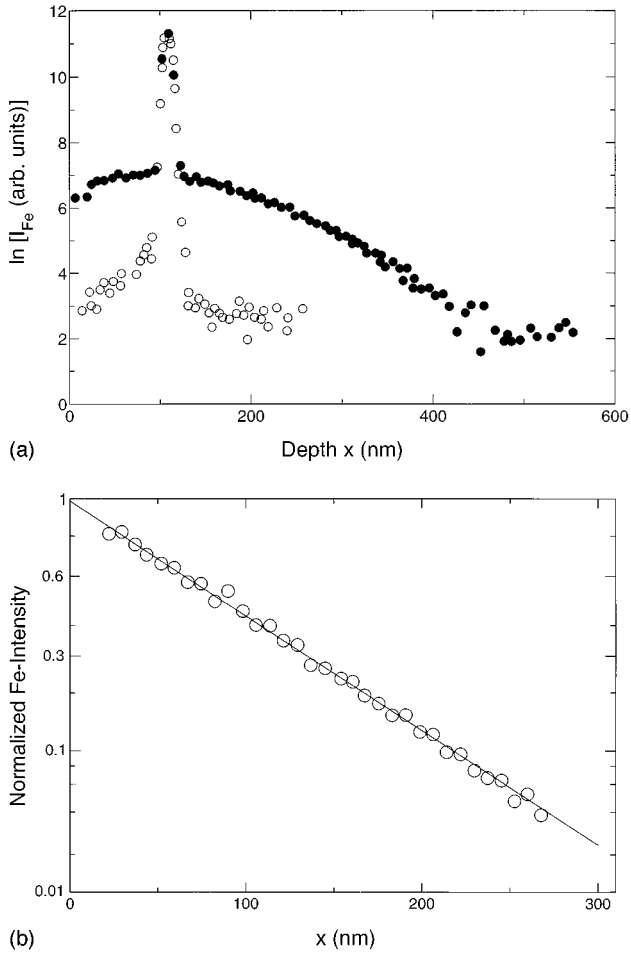

FIG. 2. (a) Typical depth profile of a Cu/Fe/Cu sandwich specimen (● after diffusion annealing for 6420 s at 801 K; ○ as prepared). (b) Probability plot [erfc^{-1}c vs x, cf. Eq. (5) of text] of the same data. The depth is measured from the intensity maximum in (a).

with an accuracy of ± 2 K. During annealing the temperature was constant within ± 0.5 K. The diffusion annealing was performed in a resistance furnace. Therefore it was necessary to consider properly the heating and cooling times for a determination of the effective annealing times. This was performed using the procedure described in Ref. 9.

The depth distribution of the Fe and Ni tracers was measured for every specimen before and after the diffusion treatment by sputter erosion combined with secondary-ion mass spectrometry. The measured SIMS intensity is supposed to be proportional to the concentration of the tracer. Uniform erosion with a rate of about 0.05 nm/s was achieved by scanning a 100 μm diameter ion beam of 4 keV O_2^+ over an area of about 1×1 mm^2 in a commercial SIMS apparatus (ATOMIKA). In order to avoid rim effects of the eroded crater an electronic aperture was set so that only those secondary ions which were emitted from the inner part of the sputtered area were detected. Under these conditions impurity concentrations of about 10 ppm Fe and 25 ppm Ni could be detected. The depth of the sputter craters was measured by mechanical probing (DEKTAK 3030) after sectioning was completed. This resulted for each sample in an individual scaling factor for the conversion of integrated flux of sputter ions to depth. As a compromise between the accuracy of the depth measurement and reasonable sputter times, craters were eroded always to a depth of about 800 nm, which could be measured in most cases with an accuracy of better than $\pm 15\%$. These error limits arise mainly from the wavy structure of the sample surface. The diffusion coefficients of this work were determined with an accuracy of between 16% and 55% in the case of Ni diffusion, and between 12% and 32% for Fe diffusion. The main contribution to this uncertainty results from that of the depth calibration.

III. RESULTS

Figures 1 and 2 show typical concentration depth profiles of Ni-Cu and Fe-Cu sandwich specimens, respectively. After diffusion the maximum concentration is distinctly reduced in the Ni-Cu sandwich [Fig. 1(a)] in accordance with the high solubility of Ni in copper. This is not observed in the Fe-Cu sandwich [Fig. 2(a)] because of the limited solubility of Fe in copper at these annealing temperatures. In this case the de-

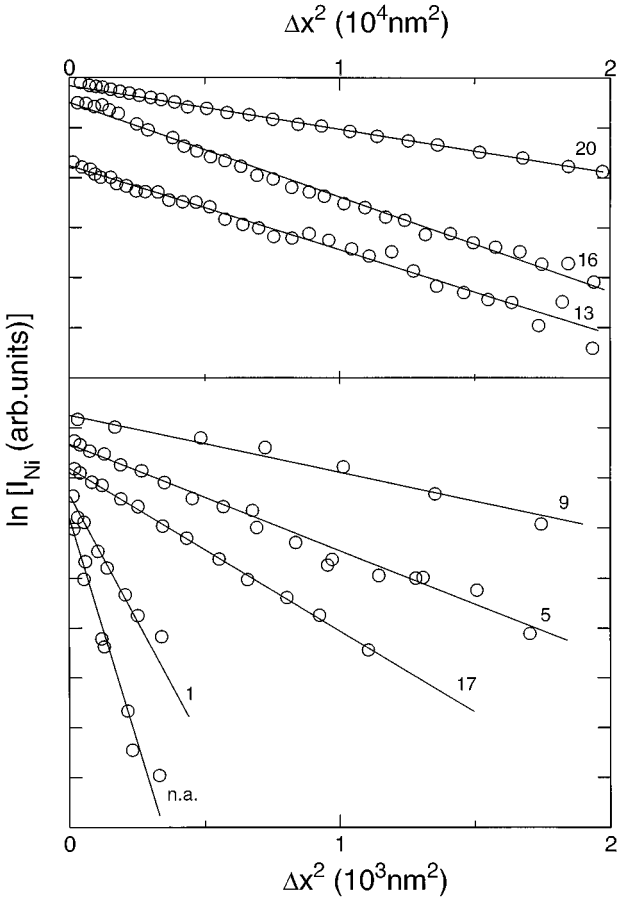

FIG. 3. Concentration depth profiles of Ni after diffusion annealing in the form of ln$c$ vs Δx^2. The numbers refer to Table I; the label ''n.a.'' indicates the nonannealed condition. The solid lines are fitted curves according to Eq. (2).

TABLE I. Diffusion coefficients of Ni in copper.

No.	T (K)	t (s)	D ($m^2\,s^{-1}$)	$\Delta D/D$ (%)
1	613	2.46×10^{6}	4.67×10^{-24}	23
2	622	2.12×10^{6}	8.32×10^{-24}	35
3	637	6.17×10^{5}	2.10×10^{-23}	16
4	659	7.74×10^{5}	1.25×10^{-22}	25
5	659	7.74×10^{5}	1.50×10^{-22}	33
6	685.5	9.22×10^{5}	4.00×10^{-22}	40
7	698	1.76×10^{5}	9.11×10^{-22}	27
8	698	1.76×10^{5}	1.12×10^{-21}	23
9	705	1.59×10^{5}	1.36×10^{-21}	27
10	705	1.59×10^{5}	2.37×10^{-21}	16
11	732.5	2.04×10^{5}	4.28×10^{-21}	52
12	735	5.83×10^{5}	7.15×10^{-21}	43
13	750	8.76×10^{4}	1.68×10^{-20}	42
14	766.5	1.71×10^{4}	3.75×10^{-20}	33
15	782.5	9.48×10^{3}	9.86×10^{-20}	32
16	801	6.60×10^{3}	1.44×10^{-19}	46
17	849	7.34×10^{1}	9.25×10^{-19}	28
18	872	6.53×10^{1}	3.05×10^{-18}	55
19	921.5	9.38×10^{1}	1.08×10^{-17}	24
20	949	1.12×10^{2}	2.22×10^{-17}	44

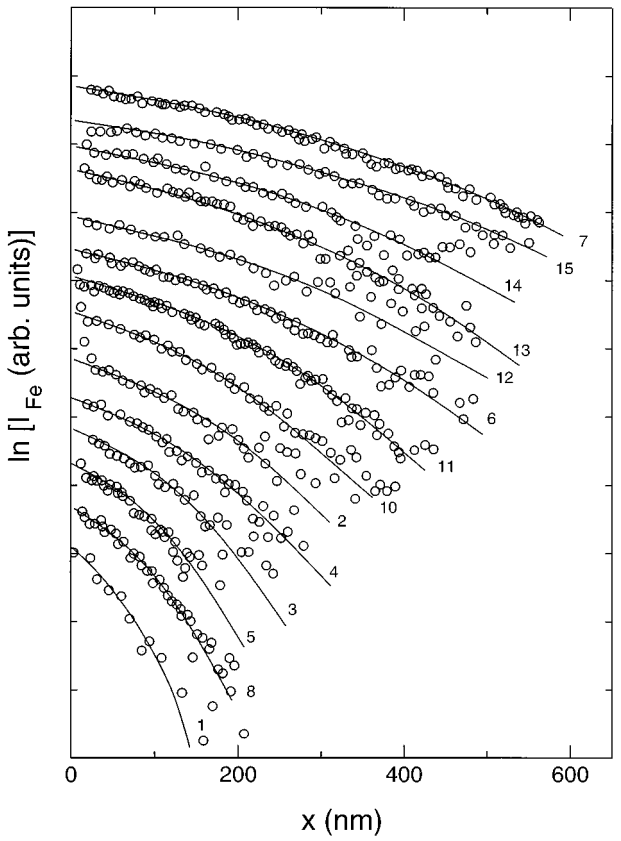

FIG. 4. Concentration depth profiles of Fe after diffusion annealing in the form of ln$c$ vs x. The numbers refer to Table II; the solid lines are fitted curves according to Eq. (5).

posited layer serves as a constant source of Fe atoms.

The solution of Fick's second law depends on the boundary conditions. For a sufficiently thin starting layer of a completely soluble impurity the penetration profiles obey the ''thin-film'' solution, i.e., the spatiotemporal concentration distribution $c(x,t)$ of the diffusing element is given by[10]

$$c(x,t)=A(\pi Dt)^{-1/2}\exp(-\Delta x^2/4Dt), \qquad (2)$$

TABLE II. Diffusion coefficients of Fe in copper.

No.	T (K)	t (s)	D ($m^2\,s^{-1}$)	Δ/D (%)
1	651	6.05×10^{5}	1.96×10^{-21}	28
2	663	2.07×10^{6}	3.35×10^{-21}	23
3	680	4.95×10^{5}	4.59×10^{-21}	23
4	691	2.75×10^{5}	1.98×10^{-20}	29
5	704	1.32×10^{5}	2.34×10^{-20}	32
6	719	2.45×10^{5}	5.93×10^{-20}	20
7	741	2.64×10^{5}	1.15×10^{-19}	26
8	756	7.45×10^{3}	2.80×10^{-19}	22
9[a]	787	3.25×10^{3}	9.53×10^{-19}	15
10	801	6.06×10^{3}	1.40×10^{-18}	12
11	830	2.76×10^{3}	4.14×10^{-18}	18
12	843	2.23×10^{3}	6.95×10^{-18}	30
13	843	2.23×10^{3}	7.80×10^{-18}	14
14	850	2.35×10^{3}	8.81×10^{-18}	14
15	870	1.93×10^{3}	1.55×10^{-17}	20

[a]Gaussian distribution (see text).

TABLE III. Diffusion of Fe in copper.

Temperature (K)	D^0 (10^{-4} m^2 s^{-1})	Q (eV)	Ref.
1104–1347	1.4±0.28	2.25±0.02	14
990–1329	1.01±0.23	2.21±0.02	15
990–1347	1.03±0.14	2.21±0.015	14, 15
733–1343	1.36	2.26±0.04	16
1005–1297	1.3	2.23	17
1063–1274	1.13±0.23	2.22±0.01	18
651–870	0.10±0.03	2.04±0.02	present results disregarding D (691 K)

TABLE IV. Diffusion of Ni in copper.

Temperature (K)	D^0 (10^{-4} m^2 s^{-1})	Q (eV)	Ref.
1016–1349	2.7±0.4	2.45±0.015	14
968–1334	3.8±0.2	2.46±0.005	19
1172–1340	$1.7^{+1.0}_{-0.6}$	2.40±0.05	20
1128–1328	$1.93^{+0.73}_{-0.5}$	2.41±0.035	21
1016–1349	$2.72^{+0.46}_{-0.40}$	2.45±0.015	14, 20, 21
613–949	$0.62^{+0.31}_{-0.21}$	2.32±0.025	present results disregarding D (732.5 K)

where $\Delta x=(x-x_0)$ is the distance measured from the initial position of the deposited thin layer, t is the diffusion time, D is the diffusion coefficient, and A is the total amount of the tracer or impurity. The concentration depth profiles of Ni were analyzed on the basis of Eq. (2) assuming that the concentration c is proportional to the measured SIMS intensity of the impurity. Typical penetration profiles are presented in the usual form of ln$c$ vs Δx^2 in Fig. 3. The diffusion coefficients of Ni were determined from the slopes s and s_0 of the straight lines which were fitted to the penetration curves before and after diffusion annealing for a time t, respectively, by a least squares fit procedure after background correction. The diffusion coefficients D are calculated from the relation[10]

$$D=(1/s-1/s_0)/4t. \tag{3}$$

Two features are worth noticing from the penetration plots: (i) the curves bend up in the vicinity of the concentration maximum, i.e., at $\Delta x=0$, and (ii) a slight overall curvature is visible which is most pronounced in the plot of the nonannealed specimen. The first feature pertaining to the enhanced intensity in the vicinity of the concentration maximum is attributed to an enhancement in the ionization probability during SIMS analysis. This enhancement arises probably due to contamination with the residual gas atmosphere (mainly oxygen, nitrogen, and water vapor in the pressure range of $<10^{-6}$ Pa) during specimen preparation in

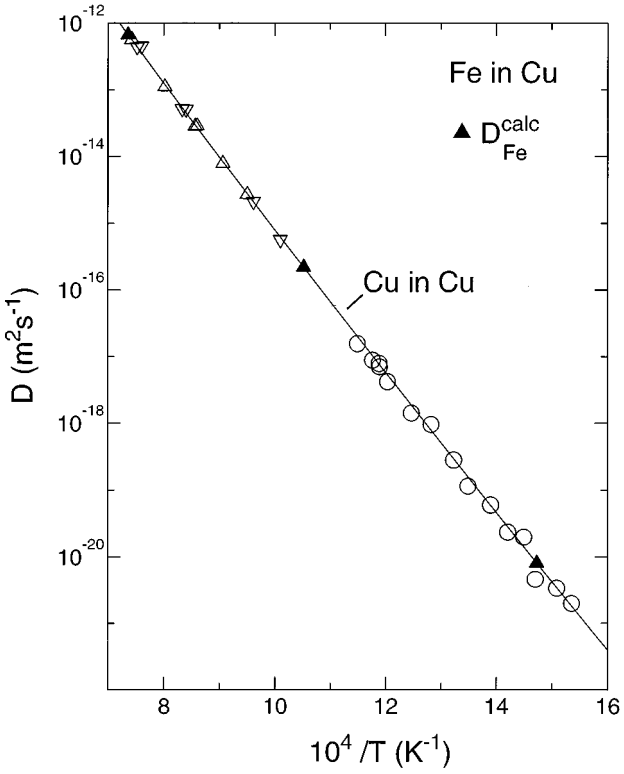

FIG. 5. Arrhenius plot of Fe diffusion in copper: △, Mackliet (Ref. 14); ▽, Mullen (Ref. 15); ○, present results. The solid line represents the two-exponential fit of copper self-diffusion according to Ref. 23. The calculated D_{Fe} values are obtained with the aid of the modified electrostatic model (Ref. 1) using $\Delta Z_{eff}=0$.

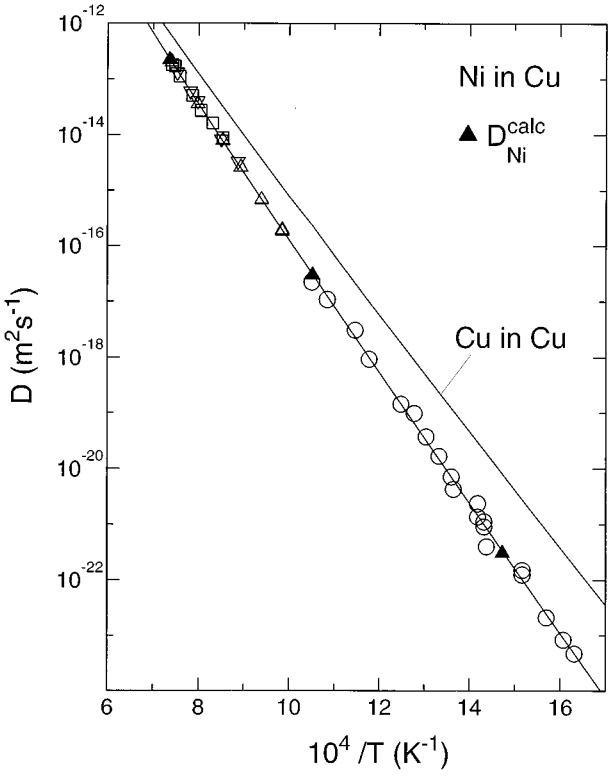

FIG. 6. Arrhenius plot of Ni diffusion in copper: △, Mackliet (Ref. 14); □, Monma, Suto, and Oikawa (Ref. 20); ▽, Anusavice *et al.* (Ref. 21); ○, present results. The solid lines represent the two-exponential fit to copper self-diffusion according to Ref. 23 and to the experimental data of Ni diffusion. The calculated D_{Ni} values are obtained with the aid of the modified electrostatic model (Ref. 1) using $\Delta Z_{eff}=-0.6$.

the UHV chamber.[11] As such contamination has no effect on the diffusion of the impurity atom outside the contaminated zone, data were always evaluated there. The other noteworthy feature relating to the slight curvature in some of the Gaussian plots arises due to atomic mixing effects during the sputter sectioning process, which are known to produce exponentially decaying concentration profiles.[12]

The derived diffusion coefficients D_{Ni} together with their relative uncertainties are listed in Table I. Here the results of former measurements[13] are also included. The temperature dependence of the diffusion coefficient evaluated by a least squares fit is given by

$$D_{\mathrm{Ni}}=(0.62^{+0.31}_{-0.21})\times 10^{-4} \times \exp(-2.32\pm 0.025\ \ \mathrm{eV}/kT)\ \ \mathrm{m}^2\ \mathrm{s}^{-1}. \qquad (4)$$

In the case of a low solubility limit c_s of the impurity, e.g., of Fe in copper at the temperatures of investigation, the penetration profiles obey an error function solution of Fick's second law,[10] i.e.,

$$c(x,t)=c_s[1-\mathrm{erf}(x/2\sqrt{Dt})] \qquad (5)$$

even for thin starting layers. Figure 4 shows the penetration profiles of Fe in the ln$c$ vs x plot. The diffusion coefficients are evaluated by fitting Eq. (5) to the data, and they are listed in Table II together with their relative uncertainties. Only in specimen 9 was the amount of Fe so small that during the annealing at 787 K the concentration dropped below the solubility limit and the penetration plot was of Gaussian type. A least squares fit yields for these diffusion coefficients

$$D_{\mathrm{Fe}}=(0.10\pm 0.03)\times 10^{-4} \times \exp(-2.04\pm 0.02\ \ \mathrm{eV}/kT)\ \ \mathrm{m}^2\ \mathrm{s}^{-1}. \qquad (6)$$

IV. DISCUSSION

Many tracer diffusion measurements have been performed for Fe and Ni in copper at temperatures above about $0.7T_m$ (T_m is the melting temperature). For Fe in copper these measurements resulted in diffusion parameters D^0 and Q with little scatter (cf. Table III). The most reliable data are those obtained by Mackliet[14] and Mullen.[15] No experimental details are given in the reports of Barreau, Brunel, and Cizeron,[16] and of Bernardini and Cabane.[17] Sen, Dutt, and Barua[18] have used the less precise resistometric method for the determination of D. A combined fit of the data of Mackliet[14] and Mullen[15] results in diffusion parameters close to those of Mullen[15] (line 3 in Table III). The present results are given in the last line of Table III. A comparison of these data with those obtained at higher temperatures indicates a curvature in the Arrhenius plot which is also visible in Fig. 5.

The results of the high-temperature measurements for the diffusion of Ni in copper are collected in Table IV. There is a slightly larger scatter in these data than in those for Fe diffusion. A combined fit to the data of Refs. 14, 20, and 21 results in diffusion parameters close to those of Mackliet[14] (line 5 in Table IV). Comparison of the present results (last line in Table IV) with those obtained at the higher temperatures again indicates a curvature of the Arrhenius plot which is shown in Fig. 6. For reasons of completeness also the

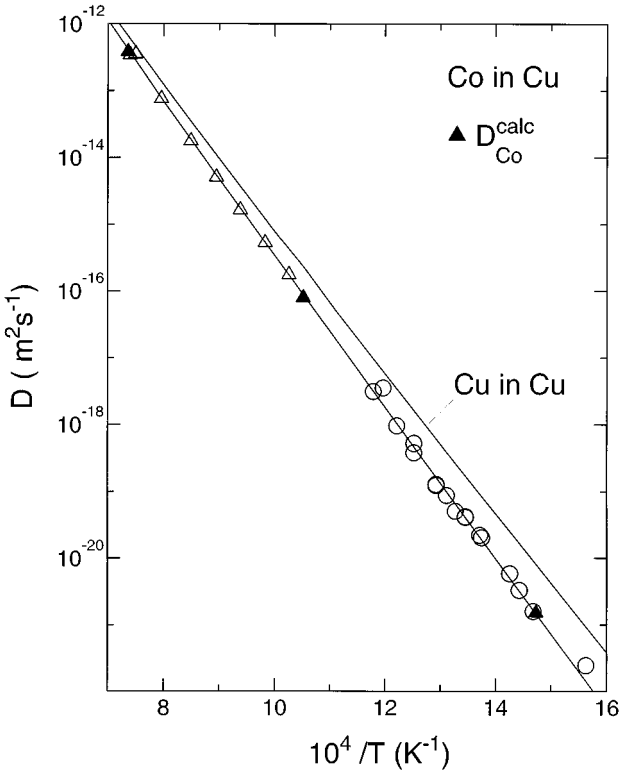

FIG. 7. Arrhenius plot of Co diffusion in copper: △, Mackliet (Ref. 14); ○, Döhl, Macht, and Naundorf (Ref. 11). The solid lines represent the two-exponential fit to copper self-diffusion according to Ref. 23 and to the experimental data of Co diffusion (Ref. 24). The calculated D_{Co} values are obtained with the aid of the modified electrostatic model (Ref. 1) using $\Delta Z_{\mathrm{eff}}=-0.35$.

Arrhenius plot of Co diffusion in copper,[11,14] is shown in Fig. 7. One recognizes that the diffusivity of Fe is close to that of copper self-diffusion, and that the diffusivity decreases when going from Fe to Ni.

Curved Arrhenius plots can be described using Eq. (1). This two-exponential fit to the experimental data in Figs. 5–7 was performed with the Morrison routine[22] and the results of these fits are listed in Table V. For Fe the most reliable data of Refs. 14 and 15 are analyzed together with the present results. In this analysis weights of 1 and 1/3 for the high- and low-temperature data, respectively, are used as deduced from the statistical deviations of about ±3% and ±10%, respectively. For Ni diffusion in copper the high-temperature data of Refs. 14, 20, and 21 are analyzed together with the present results. In this case weights of 1 and 1/5, respectively, are used. For reasons of comparison the results of copper self-diffusion[23] and Co diffusion in copper[24] are also listed in Table V.

At low temperatures the divacancy concentration, and thus its contribution to D, are almost negligible. Consequently, it is expected that the activation energy Q measured at these temperatures should be close to Q_{1V} of Table V. A comparison of Q_{1V} and Q confirms this expectation for Ni (cf. Table IV) and for Co diffusion in copper.[24] The activation energy Q_{1V} derived for Fe diffusion in copper with the lowest standard deviation σ is about 0.2 eV lower than the low-temperature activation energy Q from Table III. This would result in a relative divacancy contribution D_{2V}/D of

TABLE V. Parameters of the two-exponential fit.

System	No. of data points (high-T; low-T range)	Weights	Standard deviation σ	D^0_{1V} (10^{-4} m^2 s^{-1})	Q_{1V} (eV)	D^0_{2V} (10^{-4} m^2 s^{-1})	Q_{2V} (eV)	D_{2V}/D (at T_m)
Cu in Cu Ref. 23	52 (34;18)	1;1/3	0.054	$0.13^{+0.08}_{-0.05}$	2.05±0.025	$4.5^{+5.7}_{-2.5}$	2.46±0.12	0.51∓0.12
Fe in Cu	27 (12;15)	1;1/3	0.072	$[(1.9^{+16}_{-1.7})\times10^{-3}]$	(1.82±0.12)	$(1.57^{+0.77}_{-0.52})$	(2.26±0.12)	(0.95)
Co in Cu Ref. 24	24 (8;16)	1;1/5	0.077	$0.74^{+0.22}_{-0.17}$	2.25±0.02	$7.36^{+2.9\times10^6}_{-735.8}$	3.24±1.0	0.18∓0.08
Ni in Cu	38 (19;19)	1;1/5	0.103	$0.56^{+0.46}_{-0.25}$	2.32±0.035	48^{+1070}_{-16}	2.90±0.42	0.37∓0.17

95% at T_m, and of 31% at $T_m/2$. Both values appear to be distinctly too high. At low temperatures the divacancy contribution to D is close to zero. At T_m $D_{2V}/D_{1V}=1$ holds for self-diffusion.[21] In this sense the evaluated $D_{2V}/D_{1V}=19$ for Fe diffusion in copper is definitely too high. Therefore it must be concluded that the parameters given in Table V for Fe diffusion in copper do not reflect the true D_{2V}/D_{1V} ratio.

A comparison of the experimental data with the hitherto proposed theoretical models of impurity diffusion in noble metals[3,5] is restricted to the temperature range from $0.7T_m$ to T_m. Therefore in the following the characteristic values Q_{85} and ΔQ_{85} will be used, which refer to the activation energy of impurity diffusion and to its deviation from the activation energy of self-diffusion, respectively, at an average temperature of $0.85T_m$. The results of the comparison are listed in Table VI. The original electrostatic model,[3] where the charge difference ΔZ is equal to the difference of the columns of the periodic system, leads to a distinct overestimation of ΔQ_{85} (cf. ΔQ_E in column 4 of Table VI). For Fe, Co, and Ni in copper effective ΔZ's were estimated from the magnetic properties of dilute alloys.[3] Using these ΔZ_{eff} values the agreement between experimental and calculated ΔQ_{85} is considerably improved (cf. $\Delta Q_{E_{\text{eff}}}$ in column 5 of Table VI). The original T_m model[5] reveals good agreement for Co. For Fe (Ni), however, a marked overestimation (underestimation) of ΔQ_{85} has to be noted (cf. ΔQ_{T_m} in column 6 of Table VI). Iijima, Hoshino, and Hirano[25] have used an oscillating potential for the calculation of ΔQ_{85}. In this approach the temperature dependence of the correlation factor is considerably overestimated, so that the calculated ΔQ cannot be used for a comparison with the experimental data. Adams, Foiles, and Wolfer[26] have applied the embedded-atom method (EAM) in order to calculate ΔQ for various impurity diffusion systems. For Ni diffusion in copper the calculated $\Delta Q_{85}=0.17$ eV is not far from that obtained with the aid of the T_m model.

The complete temperature function of the impurity diffusion coefficient according to Eq. (1) can be calculated with the aid of the modified electrostatic model.[1] This includes divacancy contributions[7] and assumptions concerning the diffusion entropy and lattice frequencies. Furthermore, effective values of ΔZ have to be supplied. The best fit to the experimental $D(T)$ is obtained for Fe, Co, and Ni diffusion in copper using $\Delta Z(\text{Fe})=0$, $\Delta Z(\text{Co})=-0.35$, and $\Delta Z(\text{Ni})=-0.6$ (cf. Table VII and the solid lines in Figs. 5–7). In Fig. 5 D(Cu) and D(Fe) are nearly identical. The fitting values of ΔZ are near those estimated by Le Claire[3] (cf. Table VI). $\Delta Z(\text{Fe})=0$ corresponds to the expected $3d^7$ ground state for Fe in copper.[27] In this connection it may be mentioned that Mott[28] has assumed about 0.9, 0.9, and 0.5 electrons in the s band of Fe, Co, and Ni, respectively, which corresponds to $\Delta Z(\text{Fe})\approx\Delta Z(\text{Co})\approx-0.1$ and $\Delta Z(\text{Ni})\approx-0.5$.

In the modified E model the binding energy between impurity and vacancy in copper is estimated to be about $\Delta H^F_{1V}=0.195\Delta H^M_{1V}$.[1] For Fe, Co, and Ni in copper (cf. Table VII) this corresponds to $\Delta H^F_{1V}(\text{Fe})=0$ eV, $\Delta H^F_{1V}(\text{Co})=0.022$ eV, and $\Delta H^F_{1V}(\text{Ni})=0.042$ eV.[1] Recent *ab initio* calculations of ΔH^F_{1V} using the Korringa-Kohn-Rostoker (KKR) Green's-function method[29] arrived at distinctly larger values, i.e., $\Delta H^F_{1V}(\text{Fe})=0.08$ eV, $\Delta H^F_{1V}(\text{Co})=0.13$ eV, and $\Delta\text{H}^{\text{F}}_{1V}(\text{Ni})=0.10$ eV. The binding energies for electropositive impurities in copper and silver[29] were also found to be considerably larger than those estimated with the aid of the modified electrostatic model.[1] For these systems model calculations demonstrate that the large binding energies result in distinctly too large diffusion coefficients.[1]

TABLE VI. Comparison of experimental and calculated ΔQ_{85} (eV) for Fe, Co, and Ni diffusion in copper using the hitherto proposed models.

Metal	Q^{expt}_{85} (eV)	$\Delta Q^{\text{expt}}_{85}$ (eV)	ΔQ_E (eV)[a]	$\Delta Q_{E_{\text{eff}}}$ (eV)[b]	ΔQ_{T_m} (eV)[c]	Ref.
Cu	2.20					23
Fe	2.21	+0.01	+2.41	+0.09	+0.17	14,15
Co	2.35	+0.15	+1.27	+0.21	+0.16	14
Ni	2.45	+0.25	+0.47	+0.32	+0.14	14

[a]E=electrostatic model (Ref. 3), using $\Delta Z=-3$, -2, and -1, for Fe, Co, and Ni; respectively.
[b]E_{eff}=electrostatic model (Ref. 3), using $\Delta Z_{\text{eff}}=-0.25$, -0.5, and -0.75, for Fe, Co, and Ni, respectively.
[c]$T_m=T_m$ model (Ref. 5).

TABLE VII. Comparison of experimental diffusion parameters with results of model calculations. The calculations were performed with the aid of the modified electrostatic model (Ref. 1) using effective charge differences ΔZ_{eff}.

System	ΔZ_{eff}	ΔH_{1V}^{M} (eV)[a]	D_{85}^{0} (10^{-4} m^2 s^{-1})	Q_{85} (eV)	$D(T_m)$, extrap. (10^{-13} m^2 s^{-1})	D_{1V}^{0} (10^{-4} m^2 s^{-1})	Q_{1V} (eV)	$D(0.5T_m)$ (10^{-21} m^2 s^{-1})
Cu in Cu (expt.)			0.89	2.20	6.1	0.131	2.05	7.5
Fe in Cu (calc.)	0	0	0.91	2.20	6.4	0.139	2.05	7.9
(expt.)			1.03	2.21	6.4	(0.10)[b]	(2.04)[b]	8.1
Cu in Cu (calc.)	−0.35	0.114	(1.91)[c]	(2.35)[c]	(3.7)[c]	0.28	2.21	1.5
(expt.)			(1.93)[c]	(2.35)[c]	(3.8)[c]	0.74	2.25	1.5
						(0.43)[d]	(2.22)[d]	(1.4)[d]
Ni in Cu (calc.)	−0.6	0.216	2.4	2.44	2.2	0.40	2.31	0.31
(expt.)			2.7	2.45	2.2	0.56	2.32	0.36

[a]Difference of the vacancy migration energies of impurity and host.
[b]Experimental data from Table III.
[c]Valid for $\overline{T}/T_m=0.93$. Calculated values for $\overline{T}/T_m=0.85$ are $D_{85}^{0}=1.46\times10^{-4}$ m^2 s^{-1} and $Q_{85}=2.32$ eV.
[d]Experimental data from Ref. 11.

V. CONCLUSION

The present results for the diffusion of Fe and Ni in copper in the temperature range between about $0.45T_m$ and $0.7T_m$ are compatible with earlier tracer diffusion data in the higher-temperature range. The resulting curved Arrhenius plots are interpreted as the combined effect of monovacancy and divacancy diffusion. The obtained temperature functions of the diffusion coefficients can be described with the aid of the modified electrostatic model of impurity diffusion when using effective values for the charge difference between host atom and impurity.

ACKNOWLEDGMENTS

This study was partially supported by the Deutsche Forschungsgemeinschaft. The assistance of I. Dencks in the preparation of the samples is gratefully acknowledged.

*Present address: Centre de Recherches en Physique des Plasma, Vilingen, Switzerland.

[1] G. Neumann and V. Tölle, Philos. Mag. A **71**, 231 (1995); **71**, 249 (1995).
[2] A. D. Le Claire and A. B. Lidiard, Philos. Mag. **1**, 518 (1956).
[3] A. D. Le Claire, Philos. Mag. **7**, 141 (1962).
[4] D. Lazarus, Phys. Rev. **93**, 973 (1954).
[5] G. Neumann and W. Hirschwald, Phys. Status Solidi B **55**, 99 (1973).
[6] G. Neumann and W. Hirschwald, Z. Phys. Chem. N.F. **89**, 309 (1974).
[7] G. Neumann, Phys. Status Solidi B **144**, 329 (1987).
[8] M.-P. Macht and V. Naundorf, J. Appl. Phys. **53**, 7551 (1982).
[9] R. Döhl, Diploma thesis, Technical University Berlin, 1982.
[10] P. G. Shewmon, *Diffusion in Solids* (McGraw-Hill, New York, 1963).
[11] R. Döhl, M.-P. Macht, and V. Naundorf, Phys. Status Solidi A **86**, 603 (1984).
[12] M.-P. Macht, R. Willecke, and V. Naundorf, Nucl. Instrum. Methods Phys. Res. Sect. B **43**, 507 (1989).
[13] M.-P. Macht, V. Naundorf, and R. Döhl, in *DIMETA-82, Diffusion in Metals and Alloys*, edited by F. J. Kedves and D. L. Beke, Diffusion and Defects Monograph Series Vol. 7 (Trans. Tech., Aedermauusdorf, Switzerland,1983), p. 516.
[14] C. A. Mackliet, Phys. Rev. **109**, 1964 (1958).
[15] J. G. Mullen, Phys. Rev. **121**, 1649 (1961).
[16] G. Barreau, G. Brunel, and G. Cizeron, C. R. Acad. Sci. **272**, 618 (1971).
[17] J. Bernardini and J. Cabane, Acta Metall. **21**, 1561 (1973).
[18] S. K. Sen, M. B. Dutt, and A. K. Barua, Phys. Status Solidi A **45**, 657 (1978).
[19] A. Ikushima, J. Phys. Soc. Jpn. **14**, 1636 (1959).
[20] K. Monma, H. Suto, and H. Oikawa, J. Jpn. Inst. Met. **28**, 192 (1964).
[21] K. J. Anusavice, J. J. Pinajian, H. Oikawa, and R. T. DeHoff, Trans. AIME **242**, 2027 (1968).
[22] H. M. Morrison, Philos. Mag. **31**, 243 (1975).
[23] G. Neumann and V. Tölle, Philos. Mag. A **54**, 619 (1986).
[24] G. Neumann and V. Tölle, Philos. Mag. A **57**, 621 (1988).
[25] Y. Iijima, K. Hoshino, and K. Hirano, Metall. Trans. **8A**, 997 (1977).
[26] J. B. Adams, S. M. Foiles, and W. G. Wolfer, J. Mater. Res. **4**, 102 (1989).
[27] D. C. Abbas, T. J. Aton, and C. P. Slichter, Phys. Rev. Lett. **41**, 719 (1978).
[28] N. F. Mott, Adv. Phys. **13**, 325 (1964).
[29] U. Klemradt, B. Drittler, T. Hoshino, R. Zeller, P. H. Dederichs, and N. Stefanou, Phys. Rev. B **43**, 9487 (1991).